PRAMANA
— journal of
physics

© Indian Academy of Sciences

Vol. 86, No. 2
February 2016
pp. 479–485

Nucleon-generalized parton distributions in the light-front quark model

NEETIKA SHARMA
Indian Institute of Science Education and Research Mohali, S.A.S. Nagar, Mohali 140 306, India
E-mail: neetika@iisermohali.ac.in

DOI: 10.1007/s12043-015-1169-3; ***e*Publication:** 12 January 2016

Abstract. We calculate the generalized parton distributions (GPDs) for the up- and down-quarks in nucleon using the effective light-front wavefunction. The results obtained for GPDs in momentum and impact parameter space are comparable with phenomenological parametrization methods.

Keywords. Eelectromagnetic form factors; properties of baryons; Compton scattering by hadrons.

PACS Nos 13.40.Gp; 14.20.Dh; 13.60.Fz

1. Introduction

Generalized parton distributions (GPDs) are the important set of parameters that give us essential information about the non-perturbative structure of hadrons. GPDs have gained a lot of theoretical and experimental interest in the recent past. At the leading order, there are two GPDs: helicity-dependent $H(x, \zeta, t)$ and helicity-independent $E(x, \zeta, t)$. These are functions of three variables, namely, longitudinal momentum fraction (x), square of the total momentum transferred (t), and skewness (ζ), which represents the longitudinal momentum transferred in the process. GPDs are experimentally extracted from hard exclusive processes such as deeply virtual Compton scattering and vector meson production [1]. Recent measurements at DESY [2] and Jefferson Lab [3] will significantly advance our knowledge about the GPDs.

GPDs are expressed as off-forward matrix elements of bilocal light-front current in the overlap representation. Their first moments are related to form factors and they do not have probabilistic interpretation. For the zero skewness, the Fourier transform (FT) of the GPDs with respect to the momentum transfer in the transverse direction, gives the impact parameter-dependent GPDs. The impact parameter GPDs have probabilistic interpretation [4] and provide us information about partonic distributions in the impact parameter or transverse position space [5].

The AdS/CFT is the correspondence between the string theory on a higher-dimensional anti-de Sitter (AdS) space to conformal field theory in physical space–time [6]. This conjecture has led to a semiclassical approximation for strongly-coupled quantum field theories which provides physical insights into its non-perturbative dynamics of hadrons [7]. These models incorporate colour confinement and chiral symmetry breaking, and successfully explain the hadron spectra, e.g., the mass spectra [8], form factors [9], distribution amplitudes, etc. [10]. The idea of matching the matrix elements of AdS modes to the light-front QCD is referred to as light-front holography (LFH). This approach has been used to calculate the GPDs for valence quarks indirectly via the sum rules that connect GPDs with electromagnetic form factors (EFFs) [11].

Recently, a phenomenological light-front quark model (LFQM) has been proposed by matching the soft-wall model of AdS/QCD and light-front QCD for EFFs of hadrons with arbitrary twist dimensions [12]. LFQM successfully explains the results for hadronic form factors consistent with quark counting rules and Drell Yan–West duality. We intend to investigate the GPDs for the up- and down-quark in nucleon in the momentum and impact parameter space. The qualitative behaviour of our model predictions is compared with the recent parametrization method of parton distributions [13,14].

2. Generalized parton distributions in the light-front quark model

In the light-front formalism, the Dirac and Pauli form factors ($F_1^q(q^2)$ and $F_2^q(q^2)$) are identified by the helicity-conserving and the helicity non-conserving matrix element of the plus component of the electromagnetic current J^+. The quark EFFs in the overlap representation are defined as

$$F_1^q(t) = \int \frac{\mathrm{d}x\,\mathrm{d}^2k_\perp}{16\pi^3}[\psi^{*\uparrow}_{1/2}(x,k'_\perp)\,\psi^{\uparrow}_{1/2}(x,k_\perp)+\psi^{*\uparrow}_{-1/2}(x,k'_\perp)\,\psi^{\uparrow}_{-1/2}(x,k_\perp)]\,,$$

$$\begin{aligned} F_2^q(t) \;=\; & \frac{-2M_N}{q_1-\iota q_2}\int \frac{\mathrm{d}x\,\mathrm{d}^2k_\perp}{16\pi^3}[\psi^{*\uparrow}_{1/2}(x,k'_\perp)\,\psi^{\downarrow}_{-1/2}(x,k_\perp) \\ & +\psi^{*\uparrow}_{1/2}(x,k'_\perp)\,\psi^{\downarrow}_{-1/2}(x,k_\perp)]\,, \end{aligned}$$

where $\psi^{\lambda N}_{\lambda q}(x,\ k_\perp)$ is the LFWF describing the interaction of quark with scalar diquark to form a nucleon, $\lambda_N = \uparrow\downarrow$ correspond to the specific helicities of the nucleon, $\lambda_q = \pm 1/2$ is helicity of the struck quark, and $t = -q^2 = -q_\perp^2$ is the momentum transferred.

The quark–scalar diquark helicity component of the LFWFs are expressed as

$$\begin{aligned} \psi^{\uparrow}_{1/2}(x,k_\perp) \;&=\; \varphi_q^1(x,\ k_\perp)\,, \qquad \psi^{\uparrow}_{-1/2}(x,k_\perp) = -\left(\frac{k^1+\iota k^2}{xM_n}\right)\varphi_q^2(x,\ k_\perp)\,, \\ \psi^{\downarrow}_{1/2}(x,k_\perp) \;&=\; \left(\frac{k^1-\iota k^2}{xM_n}\right)\varphi_q^2(x,\ k_\perp)\,, \quad \psi^{\downarrow}_{-1/2}(x,k_\perp) = \varphi_q^1(x,\ k_\perp)\,, \end{aligned} \tag{1}$$

where

$$\varphi_q^i(x,\, k_\perp) = \frac{4\pi}{\kappa}\, N_q^i \sqrt{\frac{\log(1/x)}{1-x}}\, x^{a_q^i}(1-x)^{b_q^i}\, \mathrm{e}^{-\frac{k_\perp^2}{2\kappa^2}\frac{\log(1/x)}{(1-x)^2}}\,.$$

Here N_q^i is the normalization constant and a_q^i and b_q^i are the free parameters to be fitted to the experimental data on EFFs for proton and neutron.

Sum rules connect the GPDs for unpolarized quarks with the EFFs [4]

$$F_1^q(t) = \int_0^1 \mathrm{d}x\; H^q(x,t)\,, \qquad F_2^q(t) = \int_0^1 \mathrm{d}x\; E^q(x,t)\,. \tag{2}$$

We have used the standard convention to define the GPDs for valence quarks (minus antiquark) $H^q(x,t) = H^q(x,0,t) + H^q(-x,0,t)$; $E^q(x,t) = E^q(x,0,t) + E^q(-x,0,t)$. After performing the matching of respective expressions for the nucleon form factors results, the GPDs for the up- and down-quark are given as

$$\begin{aligned} H^q(x,t) &= n_q \frac{(N_q^1)^2}{I_1^q} x^{2a_q^1}(1-x)^{2b_q^1+1}\left[1+\frac{\sigma(x)^2\kappa^2}{\log(1/x)}\left(1-\frac{q_\perp^2\log(1/x)}{4\kappa^2}\right)\right] \\ &\quad\times \exp\left[-\frac{\log(1/x)}{4\kappa^2}q_\perp^2\right], \\ E^q(x,t) &= \kappa_q \frac{2N_q^1N_q^2}{I_2^q}\, x^{a_{1q}+a_{2q}-1}(1-x)^{b_{1q}+b_{2q}+2}\exp\left[-\frac{\log(1/x)}{4\kappa^2}q_\perp^2\right], \end{aligned} \tag{3}$$

where n_q is the number of valence quarks in the nucleon, κ_q is the quark anomalous magnetic moment, and

$$\sigma(x) = \frac{N_q^2}{N_q^1}\, x^{(a_q^2-a_q^1)}(1-x)^{(b_q^2-b_q^1+1)}.$$

The integrals in the above equation are defined as

$$\begin{aligned} I_1^q &= \int_0^1 \mathrm{d}x\,(N_q^1)^2\, x^{2a_q^1}(1-x)^{2b_q^1+1}\left[1+\frac{\sigma^2\kappa^2}{\log(1/x)}\right], \\ I_2^q &= 2\int_0^1 \mathrm{d}x\, N_q^1N_q^2\, x^{a_{1q}+a_{2q}-1}(1-x)^{b_{1q}+b_{2q}+2}\,. \end{aligned} \tag{4}$$

For the numerical computation of GPDs, we use the following set of parameters: $a_u^1 = 0.285$, $a_d^1 = 0.7$, $b_u^1 = 0.05$, $b_d^1 = 1$, $a_u^2 = 0.244$, $a_d^2 = 0.445$, $b_u^2 = 0.109$, $b_d^2 = 0.336$. In figures 1a and 1b, we have presented the spin-conserving GPD $H^{u/d}(x,t)$ as a function of x for $t = -0.5, -1, -2\ \mathrm{GeV}^2$ for up- and down-quarks. The overall behaviour of the GPDs is the same for up- and down-quarks. However, the fall-off behaviour is faster with increasing values of x for the down-quark. In figures 1c and 1d, we present the GPD $E^{u/d}(x,t)$ as a function of x for different values of t for the up- and down-quarks. In this case, the profile function increases to a maximum value and then decreases. However, the fall-off behaviour is almost similar for both up- and down-quarks.

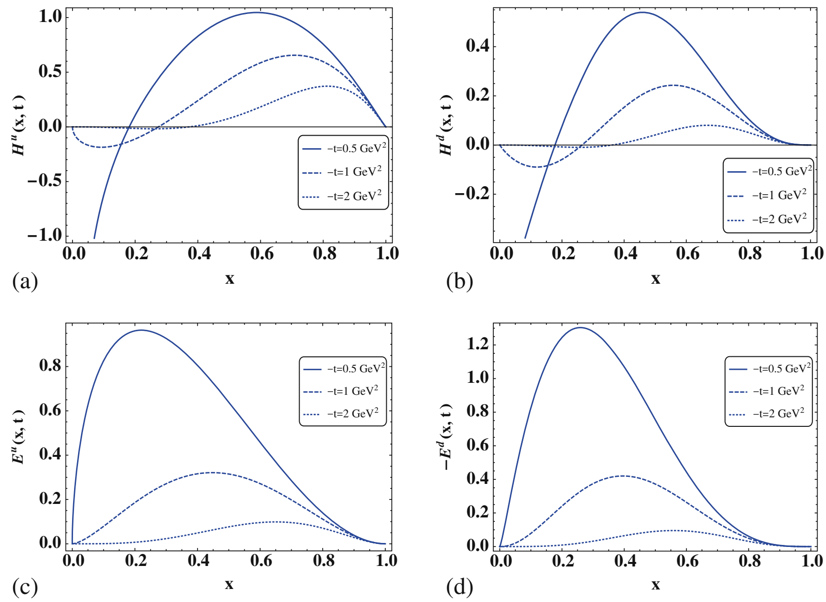

Figure 1. Plots of (**a**) $H^u(x,b)$ vs. x for fixed values of impact parameter $b = |b_\perp|$, (**b**) $H^u(x,b)$ vs. b for fixed values of x, (**c**) same as in (**a**) but for d quark and (**d**) same as in (**b**) but for d quark.

3. GPDs in impact parameter space

GPDs in the momentum space are related to the impact parameter-dependent parton distribution by the Fourier transform [5]. The transverse impact parameter $b = |b_\perp|$ is a measure of the transverse distance between the struck parton and the centre-of-momentum of the hadron. The GPDs in the impact parameter or transverse position space are

$$H^q(x,b) = \frac{1}{(2\pi)^2}\int \mathrm{d}^2 q_\perp \mathrm{e}^{-q_\perp \cdot b_\perp} H^q(x,t)\,, \tag{5}$$

$$E^q(x,b) = \frac{1}{(2\pi)^2}\int \mathrm{d}^2 q_\perp \mathrm{e}^{-q_\perp \cdot b_\perp} E^q(x,t)\,. \tag{6}$$

In order to have a comprehensive analysis of GPDs in impact parameter space, we compare our model predictions with other approaches. There are various phenomenological approaches based on the global parton analysis [14], Gaussian ansatz [15], Regge parametrization [16], etc. [17]. In a recent parametrization method (PM), the GPDs for Dirac form factor [13]

$$H^q(x,t) = q(x)\, \exp\left[1.1\frac{(1-x)^2 t}{x^{0.4}}\right], \tag{7}$$

where the quark distribution function $q(x)$

$$\begin{aligned} u(x) &= 0.262x^{-0.69}(1-x)^{3.50}(1+3.83x^{0.5}+37.65x)\,,\\ d(x) &= 0.061x^{-0.65}(1-x)^{4.03}(1+49.05x^{0.5}+8.65x)\,. \end{aligned} \tag{8}$$

Similarly, for the GPD $\mathcal{E}^q(x, t)$, we have used the representation [13]

$$E^q(x,\ t) = \mathcal{E}^q(x) \exp\left[a_{+} \frac{(1-x)^2 t}{x^{0.4}}\right]. \tag{9}$$

Here the function $\mathcal{E}^q(x)$ is expressed as

$$\mathcal{E}^u(x) = \frac{\kappa_u}{N_u}(1-x)^{\kappa_1} u(x), \qquad \mathcal{E}^d(x) = \frac{\kappa_d}{N_d}(1-x)^{\kappa_2} d(x), \tag{10}$$

with $k_1 = 1.53$, $k_2 = 0.31$, $N_u = 1.53$, $N_d = 0.946$, $\kappa_u = 1.673$, and $\kappa_d = -2.033$.

We compare the behaviour of impact parameter GPDs $H^{u/d}(x, b)$ and $E^{u/d}(x, b)$ in LFQM with the PM for both up- and down-quarks. In figure 2a, we have plotted the behaviour of $H^u(x, b)$ with x for fixed values $b = 0.3, 1\ \mathrm{GeV}^{-1}$, and in figure 2b, we have shown the behaviour of the same GPD with impact parameter b for fixed values $x = 0.3, 0.6$. In figures 2c and 2d, we plot the GPDs $H^d(x, b)$, while considering its variation with x and b for the same set of parameters for the down-quark. Similar plots showing the behaviour of GPDs $E^{u/d}(x, b)$ are shown in figure 3a–3d. In both cases, the qualitative behaviour of GPDs is almost the same for both the up- and down-quarks in the impact parameter space. The profile of GPDs in the LFQM shifted towards a lower value of x as b increases. Therefore, the transverse profile is peaked at $b = 0$ and falls off further.

The GPD $H^{u/d}(x, b)$ is peaked at a higher value of x and falls off sharply in LFQM, whereas in PM, the same GPD is peaked at a much lower x. The GPD $E^{u/d}(x, b)$ shows

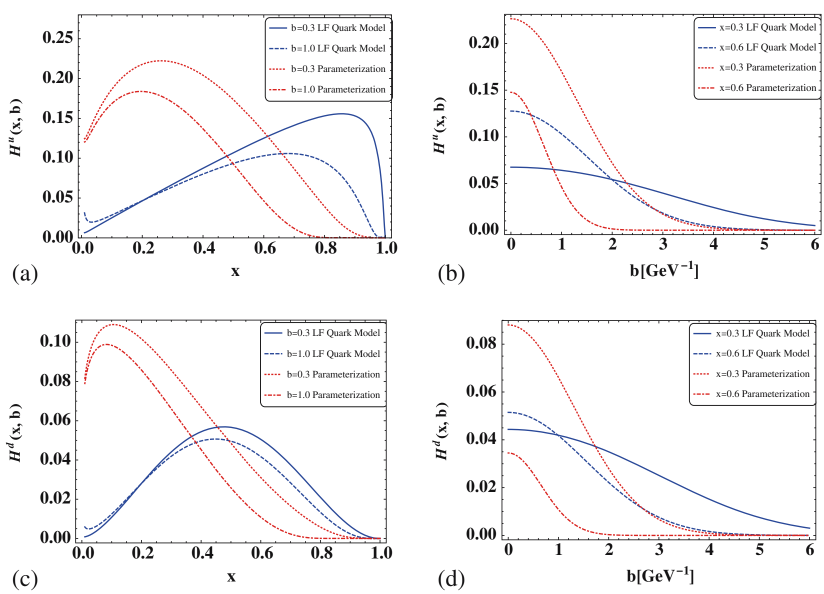

Figure 2. Plots of (**a**) $H^u(x, b)$ vs. x for fixed values of impact parameter $b = |b_\perp|$, (**b**) $H^u(x, b)$ vs. b for fixed values of x, (**c**) same as in (**a**) but for d quark and (**d**) same as in (**b**) but for d quark.

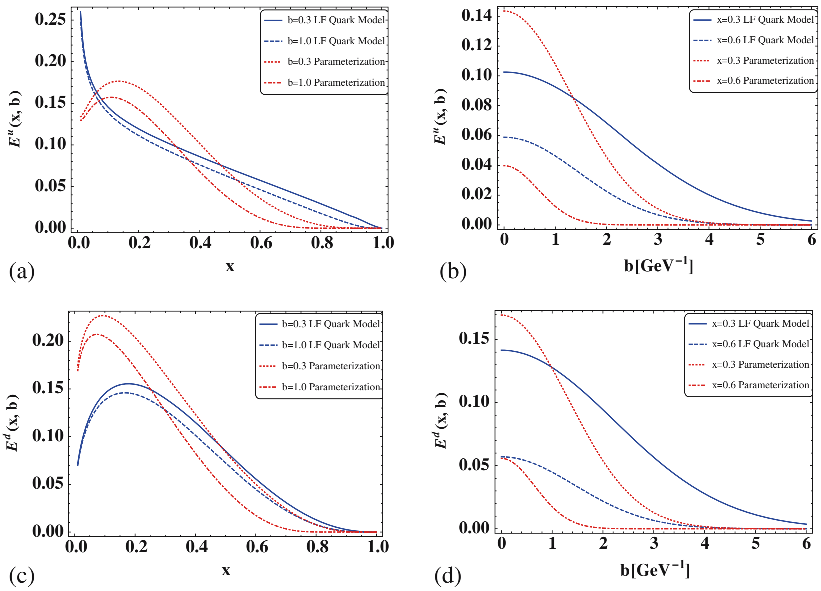

Figure 3. Plots of (**a**) $E^u(x, b)$ vs. x for fixed values of impact parameter $b = |b_\perp|$, (**b**) $E^u(x, b)$ vs. b for fixed values of x, (**c**) same as in (**a**) but for d quark and (**d**) same as in (**b**) but for d quark.

almost similar behaviour with x in two approaches. However, for small values of x, GPD has a large magnitude for the up-quark in LFQM. The small difference in the behaviour of GPDs is due to the reason that we restricted the contribution of up- and down-quarks, while the contribution of heavier quarks, such as strange and charm quarks, has been ignored. For the variation of both the GPDs, $H^{u/d}(x, b)$ and $E^{u/d}(x, b)$ with impact parameter b, the overall behaviour is the same in different models and the transverse profile is peaked at $b = 0$. It is also interesting to observe that for small values of b, the magnitude of GPD $H(x, b)$ is larger for up-quark than for down-quark, whereas the magnitude of the GPD $E(x, b)$ is marginally larger for down-quark than for up-quark.

4. Summary and conclusions

In this work, we have used a phenomenological light-front quark model to calculate the GPDs for the up- and down-quarks in nucleon. The effective light-front wavefunction is obtained by matching the matrix elements in the AdS/QCD and light-front QCD at an initial scale. A detailed analysis of nucleon GPDs has been performed in the momentum space and transverse impact parameter space. The qualitative behaviour of GPDs in transverse impact parameter space is the same as the phenomenological parametrization method, though we have considered only the valence quarks contribution. In future, we plan to generalize the LFWF to sea quarks, antiquarks, and gluons, which could then be used in the evaluation of different hadronic processes.

Acknowledgement

This work is supported by the Department of Science and Technology, Government of India (Grant No. SR/FTP/PS-057/2012).

References

[1] K Goeke, M V Polyakov and M Vanderhaeghen, *Prog. Part. Nucl. Phys.* **47**, 401 (2001)
X D Ji, *Annu. Rev. Nucl. Part. Sci.* **54**, 413 (2004)
A V Belitsky and A V Radyushkin, *Phys. Rep.* **418**, 1 (2005)

[2] HERMES Collaboration: A Airapetian *et al*, *Phys. Rev. Lett.* **87**, 182001 (2001)
ZEUS Collaboration: S Chekanov *et al*, *Phys. Lett. B* **573**, 46 (2003)

[3] CLAS Collaboration: S Stepanyan *et al*, *Phys. Rev. Lett.* **87**, 182002 (2001)

[4] X Ji, *Phys. Rev. Lett.* **78**, 610 (1997); *J. Phys. G* **24**, 1181 (1998)

[5] M Burkardt, *Phys. Rev. D* **62**, 071503 (2000); *Phys. Rev. D* **72**, 094020 (2005)

[6] J Polchinski and M J Strassler, *Phys. Rev. Lett.* **88**, 031601 (2002); *J. High Energy Phys.* **05**, 012 (2003)
A V Radyushkin, *Phys. Lett. B* **642**, 459 (2006)

[7] S J Brodsky and G F de Teramond, *Phys. Rev. Lett.* **96**, 201601 (2006); *Phys. Rev. D* **77**, 056007 (2008); **78**, 025032 (2008); *Phys. Rev. Lett.* **102**, 081601 (2009)

[8] A Vega, I Schmidt, T Branz, T Gutsche and V E Lyubovitskij, *Phys. Rev. D* **80**, 055014 (2009)
J R Forshaw and R Sandapen, *Phys. Rev. Lett.* **109**, 081601 (2012)

[9] S Hong, S Yoon and M J Strassler, *J. High Energy Phys.* **0604**, 003 (2006)
H R Grigoryan and A V Radyushkin, *Phys. Rev. D* **76**, 115007 (2007); **76**, 095007 (2007)
H J Kwee and R F Lebed, *J. High Energy Phys.* **01**, 27 (2008)

[10] Z Abidin and C E Carlson, *Phys. Rev. D* **79**, 115003 (2009)
A Vega, I Schimdt, T Gutsche and V E Lyubovitskij, *Phys. Rev. D* **83**, 036001 (2011); **85**, 096004 (2012)
T Gutsche, V E Lyubovitskij, I Schmidt and A Vega, *Phys. Rev. D* **86**, 036007 (2012)

[11] A Vega, I Schimdt, T Gutsche and V E Lyubovitskij, *Phys. Rev. D* **83**, 036001 (2011); *Phys. Rev. D* **85**, 096004 (2012)
N Sharma, *Phys. Rev. D* **90**, 095024 (2014)

[12] T Gutsche, V E Lyubovitskij, I Schmidt and A Vega, *Phys. Rev. D* **89**, 054033 (2014)

[13] O V Selyugin and O V Teryaev, *Phys. Rev. D* **79**, 033003 (2009)

[14] A D Martin, W J Stirling, R S Thorne and G Watt, *Eur. Phys. J. C* **63**, 189 (2009)

[15] A V Radyushkin, *Phys. Rev. D* **58**, 114008 (1998)
M Guidal, M V Polyakov, A V Radyushkin and M Vanderhaeghen, *Phys. Rev. D* **72**, 054013 (2005)

[16] K Goeke, M V Polyakov and M Vanderhaeghen, *Prog. Part. Nucl. Phys.* **47**, 401 (2001)

[17] F Yuan, *Phys. Rev. D* **69**, 051501(R) (2004)
L Jenkovszky, *Phys. Rev. D* **74**, 114026 (2006)